Superconducting Materials for Large Scale Applications

RONALD M. SCANLAN, ALEXIS P. MALOZEMOFF, SENIOR MEMBER, IEEE, AND DAVID C. LARBALESTIER

Invited Paper

Since the 1960s, Nb–Ti (superconducting transition temperature $T_c = 9$ K) and Nb_3Sn ($T_c = 18$ K) have been the materials of choice for virtually all superconducting magnets. However, the prospects for the future changed dramatically in 1987 with the discovery of layered cuprate superconductors with T_c values that now extend up to about 135 K. Fabrication of useful conductors out of the cuprates has been difficult, but a first generation of silver-sheathed composite conductors based on $(Bi,Pb)_2Sr_2Ca_2Cu_3O_{10}$ ($T_c \sim 110$ K) has already been commercialized. Recent progress on a second generation of biaxially aligned coated conductors using the less anisotropic $YBa_2Cu_3O_7$ structure has been rapid, suggesting that it too might enter service in the near future. The discovery of superconductivity in MgB_2 below 39 K in 2001 has brought yet another candidate material to the large-scale applications mix. Two distinct markets for superconductor wires exist—the more classical low-temperature magnet applications such as particle accelerators, nuclear magnetic resonance and magnetic resonance imaging magnets, and plasma-containment magnets for fusion power, and the newer and potentially much larger market for electric power equipment, such as motors, generators, synchronous condensers, power transmission cables, transformers, and fault-current limiters for the electric utility grid. We review key properties and recent progress in these materials and assess their prospects for further development and application.

***Keywords*—$Bi_2Sr_2CaCu_2O_8$, $(Bi,Pb)_2Sr_2Ca_2Cu_3O_{10}$, BSCCO-2212, BSCCO-2223, coated conductors, MgB_2, Nb_3Sn, Nb–Ti, superconducting wires, superconductors, $YBa_2Cu_3O_{7-\delta}$, $YBa_2Cu_3O_7$ (YBCO).**

Manuscript received December 15, 2003; revised May 4, 2004.

R. M. Scanlan, retired, was with the Lawrence Berkeley National Laboratory, Berkeley, CA 94720 USA. He is now at 26a Lost Valley Drive, Orinda, CA 94563 USA (e-mail: rmscanlan@aol.com).

A. P. Malozemoff is with the American Superconductor Corporation, Westborough, MA 01581 USA (e-mail: amalozemoff@amsuper.com).

D. C. Larbalestier is with the Applied Superconductivity Center, University of Wisconsin, Madison, WI 53706–1609 USA (e-mail: larbalestier@engr.wisc.edu).

Digital Object Identifier 10.1109/JPROC.2004.833673

I. INTRODUCTION

Superconducting conductors for electric power and magnet applications are poised for major change. For about 40 years, virtually all magnets have been made out of Nb–Ti or Nb_3Sn, the cubic low-temperature superconductors (LTSs), which possess transition temperatures T_c of 9 K and 18 K, respectively [1]. In spite of the much higher T_c values of high-temperature superconductor (HTS) materials, ~90 K (BSCCO-2212 and YBCO-123) and ~110 K (BSCCO-2223), and strong progress in developing HTS wire, these materials have not yet made a serious dent in the commercial dominance of Nb–Ti and Nb_3Sn in the broader magnet market [1]. That market has for years consisted of magnetic resonance imaging (MRI) and nuclear magnetic resonance (NMR), and magnets for high-energy physics accelerators and plasma fusion devices, together with smaller niches for research magnets[1] [2]. These applications were developed with LTS conductors and are well served by their low cost, coupled with their ability to be fabricated as strong, round wires with distinct filament structures, high current density and a high superconductor fill factor.

Nb–Ti conductors were scientifically understood and commercially optimized during the 1980s. Nb–Ti is in fact the only material whose fabrication process has been effectively optimized based on a detailed scientific understanding. This understanding is still being developed for the high-field use of Nb_3Sn, especially for NMR and particle accelerator applications, with much recent progress.

Since the late 1980s, conductors made from the silver-sheathed HTSs $Bi_2Sr_2CaCu_2O_8$ (BSCCO-2212) and $(Bi,Pb)_2Sr_2Ca_2Cu_3O_{10}$ (BSCCO-2223) have been in ongoing development [1]. Although the understanding of their materials science is still limited and process optimization is for now rather empirical, they have progressed to the point of being commercially available, with acceptable

[1]See also other papers in this special issue.

mechanical properties and practical current densities in the 30–77 K range [3]. These are known as first-generation HTS wires or conductors, and they are principally directed at electric power applications, a major new market for superconductivity[2] [4]. Conductors made of BSCCO-2223 are being applied in significant prototypes of electric power equipment, including an 8-MVA reactive (MVAR) synchronous condenser [5], a 5000-hp industrial motor [5], a 5 MW high-torque ship propulsion motor [5], a 5-MVA transformer [6], and a variety of power transmission and distribution cables [7]. Very recently, a magnet of BSCCO-2212 wire has generated 5 T in a background field of 20 T, making it the highest field superconducting magnet [8], a result which clearly shows the potential of HTS materials to overtake LTS materials in magnet applications.

Simultaneously, the HTS material $RBa_2Cu_3O_7$, where R is a rare-earth atom or yttrium, has been developed in a coated conductor format [9], [10]; we will use YBCO to denote this material family, since $YBa_2Cu_3O_7$ is the most commonly used member. This technology is rapidly moving from research and development to scale-up and has already enabled a first short power cable prototype carrying a commercial-level current [11]. Coated conductors are often called second-generation HTS wires or conductors. In addition, some developmental conductors are starting to be fabricated from the recently discovered superconducting material MgB_2 [12].

The situation in 2004 is distinctly different than that of five years ago. For the first time, one can say that the Nb-based LTS conductors are approaching their limits, and that BSCCO and YBCO materials, and perhaps MgB_2, are ready to surpass LTS capabilities in higher field and higher temperature domains, thus opening up new markets.

The largest potential market for HTS conductors lies in the electric power arena and involves power transmission cables, high-power industrial and ship propulsion motors, utility generators, synchronous condensers, fault-current limiters, and transformers. Study after study, such as Vice President Cheney's Task Force on National Energy Policy [13], the Secretary of Energy's National Transmission Grid Study [14], and Grid 2030 [15], the vision of the future transmission system from the Department of Energy (DOE) Office of Electric Transmission and Distribution, have highlighted the critical reliability and capacity issues in the U.S. power grid and specifically noted the beneficial potential impact of superconducting technology in addressing these issues. The Northeast blackout of Aug. 14, 2003, has elevated calls for action. Momentum from these events is propelling HTS conductors into commercialization.

In this paper, we review key properties and technical progress in superconducting materials for large-scale applications during the last few years and assess their prospects for further development and application. We limit discussion to materials in the form of flexible, long-length wires rather than bulk pellets and rods, which have their own array of issues and applications.

[2]See also other papers in this special issue.

II. Conductor Requirements for Power and Magnet Technology

Superconducting conductors for large-scale applications are round or tape-shaped wires in which one or more superconducting filaments are embedded in a matrix consisting at least partially of a normal metal, such as Cu or Ag, which provides protection against magnetic flux jumps and thermal quenching [1], [16] (Fig. 1). Such wires must have sufficient strength to withstand conductor fabrication, coil winding, cabling, the thermal stresses of cooldown, and operational electromagnetic stresses. They must be capable of carrying operating currents, dc or ac, of hundreds of amperes and, often, of being cabled to carry thousands of amperes. In particular, the minimum critical tensile stress before loss of critical current density should be in the range of 100 MPa or higher, and minimum tensile, compressive, and bending strains before degradation must be several tenths of a percent. Engineering (total cross section) current density J_e must attain 10^4–10^5 A/cm^2 in magnetic fields which extend from $\sim$0.1 to 25 T, depending on the application. The superconductor current density J_c is J_e/f, where f is the fill fraction of superconducting material in the total conductor cross section. Operating temperatures tend to be as low as possible for ultrahigh-field ($\sim$25 T) dc applications (for example, 2 K in superfluid helium) but are as high as possible for ac power applications, since ac losses generated at low temperatures exact a stiff cooling penalty of many times the Carnot efficiency in practical cryogenic environments.

Estimates of the maximum acceptable price for different applications range from $\sim$\$1 to 100 per kiloamp-meter, where kiloamp (kA) refers to the operating current level. In particular, Nb–Ti wire typically sells for \$1/kAm but is limited to operation in the helium temperature range. HTSs operating at 20–77 K are expected to be economical for some applications in the \$10–100/kAm range. In power equipment, copper wires typically operate in the range of \$15–25/kAm; this sets a benchmark for superconducting wire. As a whole, LTS conductors are used for applications where few or no conventional alternatives exist, while HTS materials must compete against copper in electric power technology, where cost pressures are almost always significant.

III. Basic Physical Properties of Superconducting Wires

We give only a brief summary of the basic physical concepts underlying the performance of superconducting materials in conductors; these are described more extensively elsewhere [1], [9], [16], [17]. These materials exhibit superconducting properties in a region below the interdependent values of critical temperature T_c, upper critical magnetic field H_{c2}, and critical current density J_c. The maximum critical temperature for metallic LTSs is 23 K; it is 40 K for MgB_2 [12] and about 135 K for HTSs based on cuprate (copper oxide) compositions [18].

Fig. 2 presents the magnetic-field/temperature (H–T) phase diagram for the three currently commercial conductor

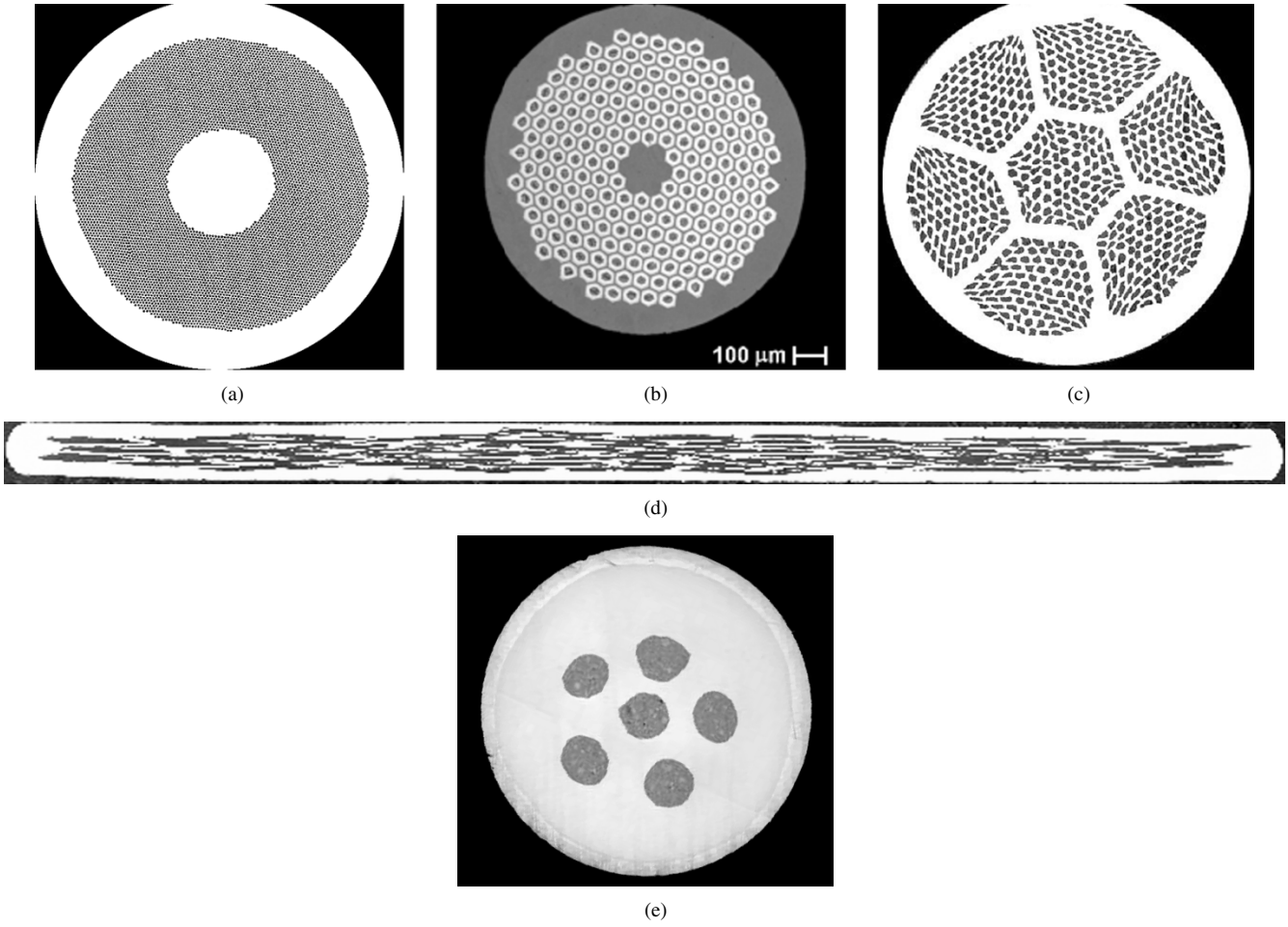

Fig. 1. Representative multifilamentary conductors made from: (a) Nb47wt.%Ti; (b) Nb_3Sn; (c) Bi-2212; (d) Bi-2223; and (e) MgB_2. The matrices for the conductors are high-purity copper for (a) and (b) and the outer sheath of (e) and pure silver or silver alloy for (c) and (d). The filaments of MgB_2 are surrounded by 316 stainless steel in (e). Conductors were manufactured by: (a) and (c) Oxford Instruments—Superconducting Technology; (b) ShapeMetal Innovation; (d) American Superconductor Corporation; and (e) Hitachi Cable in collaboration with the National Institute for Materials Science.

materials: Nb–Ti, Nb_3Sn, and $(Bi,Pb)_2Sr_2Ca_2Cu_3O_{10}$ (BSCCO-2223), and developing conductor materials: $YBa_2Cu_3O_7$ (YBCO) and MgB_2. Their very different phase diagrams result from their distinctly different crystal structures and physical parameters. All six are type II superconductors for which bulk superconductivity exists up to an upper critical field $H_{c2}(T)$, that can be highly anisotropic and exceeds 100 T for BSCCO-2223 and YBCO. However, applications of HTS materials are limited by a lower characteristic field, the so-called "irreversibility field" $H^*(T)$, at which the bulk J_c vanishes [19].

Under equilibrium conditions magnetic flux penetrates the bulk of a Type II superconductor above a lower critical field H_{c1}, which is $<$100 mT for the materials under consideration [19]. This magnetic flux exists as an array of flux-quantized line vortices or fluxons, which can be spatially ordered or disordered, static or liquid-like. Each vortex is a tube of radius of the London penetration depth $\lambda(T)$, in which superconducting screening currents circulate around a small nonsuperconducting core of radius $\xi(T)$, where $\xi(T)$ is the superconducting coherence length. The flux carried by the screening currents in each vortex equals the flux quantum $\phi_0 = 2 \times 10^{-15}$ Wb. Bulk superconductivity disappears when the normal cores overlap at the upper critical field $H_{c2}(T) = \phi_0/2\pi\mu_0\xi(T)^2$.

Type II superconductors can carry bulk current density only if there is a macroscopic fluxon density gradient defined by the Maxwell equation $\nabla \times \mathbf{B} = \mu_0\mathbf{J}$. This gradient must be sustained by the pinning of vortices at microstructural defects, and much process development is oriented to optimizing this "flux pinning" to maximize the current carrying capacity. At absolute zero, superconducting current can flow without any loss (i.e., at zero voltage) up to a critical current J_c, corresponding to the maximum pinning strength. However, at finite temperature, thermal activation can cause "flux creep" of vortices down the macroscopic fluxon density gradient (actually a small amount of creep can occur even at absolute zero because of quantum tunneling of vortices, observed in HTS materials) [19]–[21]. In most materials with random microstructural defects, the vortex structure is disordered or glassy in nature, and vortex glass theory predicts that flux creep gives rise to a $V \sim I^n$

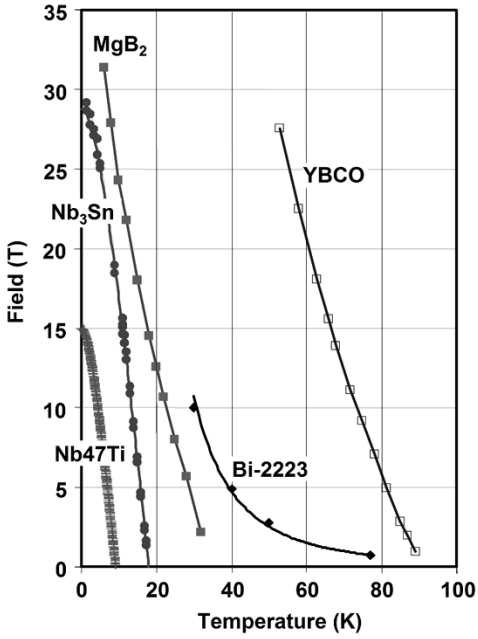

Fig. 2. Upper critical field (H_{c2}) for Nb47wt.%Ti, Nb_3Sn, and MgB_2, and irreversibility fields (H^*) for Bi-2223, and YBCO. Note that the two fields are very close for Nb47wt. %Ti, Nb_3Sn, and MgB_2, (H^* is 85%–90% of H_{c2}) but widely separated for all cuprate superconductors. For MgB_2, Bi-2223, and YBCO, the values plotted are the lower values appropriate to fields perpendicular to the strongest superconducting planes, the B planes for MgB_2 and the CuO_2 planes in the cuprates. Values plotted are the highest credible for each compound.

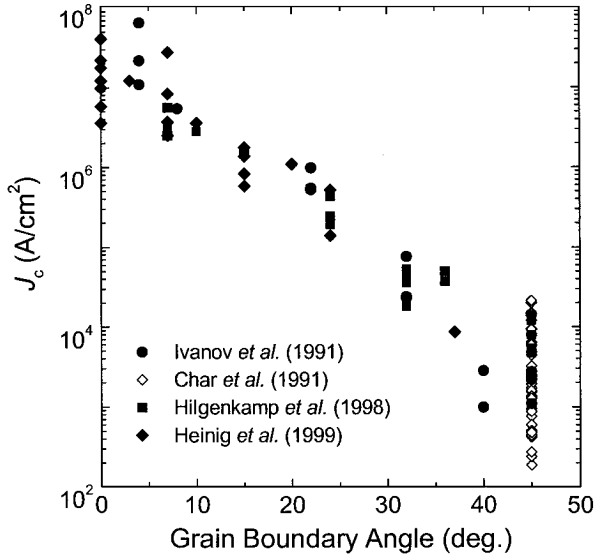

Fig. 3. Critical current density across [001] tilt grain boundaries of YBCO-123 measured at 4.2 K and self-field, from multiple studies on bicrystal boundaries [25]. The exponential falloff of J_c with grain boundary angle creates the underlying requirement for texturing to achieve high currents in HTS wires. (Based on original work of Dimos *et al.* [24]).

voltage-current relationship, where n is called the "index value" [20], [21]. Nonuniformities in material properties on nanometer or greater length scales can also give rise to this power-law relationship. The index value must be well above 30 to allow the superconducting wire to operate in a quasi-persistent mode, with minimal current decay over time. This condition can be achieved in Nb–Ti and Nb_3Sn but only rarely in HTS wires where typical index values range from 15 to 30. Because the voltage–current curve is continuous, there is no absolute measure of J_c. However, voltage increases rapidly enough with current to enable a practical definition of J_c at a characteristic electric field, typically chosen to be either 0.1 or 1 μV/cm. For magnet applications, even lower electric fields may be appropriate.

Above J_c, or at magnetic fields above a characteristic "irreversibility field" H^*, which is a function of temperature and which is much lower than H_{c2} for HTS materials, major changes occur in the vortex structure [19]. These changes have been described by a variety of theories—for example, the vortex glass melting theory, in which vortices above H^* are in an unpinned, liquid-like state. Under these conditions, current will drive a dissipative, flux-flow state, with a resistivity which, to first approximation, is given by the fraction of the material occupied by the normal cores of the vortices. This simple concept leads directly to the Bardeen–Stephen formula for flux flow resistivity $\rho_{\rm FF} = \rho_N B/\mu_0 H_{c2}$, where ρ_N is the normal state resistivity [17].

Long conductors for bulk applications are always based on polycrystalline materials, and the influence of grain boundaries is, thus, decisive. In metallic LTS and MgB_2, current flow is uniform through the polycrystalline superconducting matrix unless gross obstructions such as cracks occur. In fact, grain boundaries are often beneficial flux pinning centers, so that J_c typically increases as the grain size decreases [22].

However, HTS materials have low carrier density and short coherence lengths, factors that predispose grain boundaries to act as obstacles to current flow [23]. The most unambiguous evidence for this comes from detailed studies of YBCO films grown epitaxially on bicrystals of $SrTiO_3$ or Y_2O_3—stabilized ZrO_2 (YSZ) substrates. The critical current density J_b across the grain boundary drops exponentially below that within the grains, $J_b = J_c \exp(-\theta/\theta_c)$, as a function of the misorientation angle θ between the neighboring crystallites [24]–[26], where $\theta_c \approx 2$–5°, depending on the value of the intragrain J_c (Fig. 3).

At angles of about 10° and below, the structure of the grain boundary breaks up into identifiable edge dislocations spaced by $b/2\sin(\theta/2)$, where $b \approx 0.4$ nm is the Burgers vector. The cores of these dislocations in HTS materials are insulating. Above a misorientation angle θ of 5–7°, the spacing between the cores is less than the coherence length ξ, and the grain boundary starts to behave like a Josephson weak link. At lower misorientation angles, the dislocation cores are separated by only modestly strained material, which enables strong coupling and current flow between the grains at the bulk J_c level. The possibility of fabricating highly textured substrates coated with an epitaxial HTS layer, in which θ is small enough to permit strong coupling and, hence, significant supercurrent flow, is the basis for the coated conductor class of HTS wire [9].

The mechanism of current flow across grain boundaries in BSCCO-based conductors may be different [27], [28]. Although these materials are strongly textured around a

common c axis in wires, the in-plane orientations of their grains' ab planes are random, causing direct lateral current flow across high-angle grain boundaries to be exponentially weak. The observed current flow appears instead to involve redistribution of the current across the large-area twist boundaries separating c axis-aligned grains, allowing current to bypass high-angle grain boundaries and other obstacles.

The measurement of critical current for LTS and HTS conductors has evolved in distinctly different ways. LTS wires are always tested in magnetic fields appropriate to the application, e.g., 5–7 T for Nb–Ti and 10–15 T for Nb_3Sn at an electric field criterion that approximates magnet performance, often 0.1 μV/cm [29]. However the standard measurement for HTS materials, because of its simplicity, is in self-field at 77 K at 1 μV/cm. The drawback of this test is that J_c drops rapidly with even weak applied or self-magnetic fields, making results dependent on the conductor geometries. In the case of BSCCO-2223 conductors, proper comparison to avoid these self-field effects requires a field of at least 0.1 T at 77 K [30]. As applications develop, testing appropriate to the operating conditions will be established.

Under conditions of time-varying current and/or magnetic field, superconductors are subject to ac losses. There are three types of losses in addition to the usual eddy current losses of the normal metal matrix: 1) hysteretic, due to the motion of vortices through the superconductor; 2) interfilament "coupling" losses, due to induced currents flowing between filaments across the normal metal matrix within a multifilamentary strand; and 3) interstrand "coupling" losses, due to eddy currents flowing between the stands in a multistrand conductor (see [16]). These losses can be mitigated, but not completely eliminated, as follows. In low magnetic field environments in which the superconductor is only partially penetrated by the ac magnetic flux, the ac loss varies inversely with J_c and, therefore, can be mitigated by increasing J_c. In high-field environments in which the superconductor is fully penetrated by ac magnetic flux, hysteretic loss, normalized to the current capacity of the wire, is proportional to d, the superconductor filament diameter (or width perpendicular to the applied field), provided the filaments are decoupled. Thus, practical superconductors for ac applications are subdivided into fine filaments imbedded in a normal metal matrix so that d is reduced to a small fraction of the wire diameter (Fig. 1). Round configurations are favorable compared to tape-shaped wires, unless ac fields can be oriented along the wide face of the tapes to minimize d; round wires facilitate cabling with transposition and reduce the maximum transverse dimension as compared to a tape.

Typical multifilamentary superconductors may contain from several tens (MRI magnet) to several thousands of filaments (NMR, fusion, or accelerator magnets), with diameters from $\sim$50 to 0.1 μm, depending upon the application. For Nb–Ti, the effective filament size d_{eff} is usually the physical filament diameter. However, for Nb_3Sn and all multifilamentary HTS conductors, the effective filament size can be much larger, since the filaments may coalesce during the reaction step needed to produce Nb_3Sn, while for BSCCO-2212 or BSCCO-2223, superconducting grains grow through the Ag matrix to form a superconducting path between adjacent filaments.

Because the matrix material is typically a good normal metal such as Cu in LTS or Ag in HTS, the interfilamentary resistance is typically low enough under magnet-charging rates to allow coupling currents to flow between filaments and, thus, shield the interior of the wire from flux changes. Twisting the conductor or transposing the filaments can reduce these coupling currents, so that the magnitude of the induced electromotive force driving the currents is lessened and periodically reverses along the wire length. Typical twist pitches are ten times the wire diameter, with a ratio of five being the minimum possible. For large magnets requiring high currents, the conductor must be built up by cabling many strands together, preferably in a fully transposed geometry. The interstrand resistance then controls the magnitude of strand-to-strand coupling currents. This source of loss can be reduced by increasing the interstrand resistance, for example, by adding a high resistance alloy layer such as Cu–Ni or a Cr-plate in LTS conductors, or by applying an insulating coating to the strands.

One final issue of importance for conductor properties concerns whether current is percolative or flows uniformly through the whole cross section. For a uniform conductor, division of the measured critical current by the cross-sectional area of superconductor A_{sc} then gives the intrinsic critical current density J_c determined by the flux pinning strength of the material. For Nb–Ti and Nb_3Sn certain extrinsic defects to be described later affect the value of A_{sc} but introduce an error in calculating J_c of no more than 5%–10%. For HTS materials, this error may be much larger, because of percolative current flow arising from a combination of intrinsic obstacles like grain boundaries and extrinsic defects such as large insulating second-phase particles or cracks [9]. One of the central tasks of conductor development has been to understand such obstacles to current flow and to eliminate them as best one can, finally asking how close J_c can be brought to the ultimate possible current density, which is the depairing current density of the vortex currents J_d [17]. In Nb–Ti, which has exceptionally strong pinning, J_c is of order $0.1J_d$ [31], a value now being approached by YBCO-coated conductors under certain circumstances. However, it is always worth questioning whether the active cross section carrying current differs from the whole cross section, especially with HTS conductors and perhaps also with MgB_2 [9], [32], [33].

IV. Niobium–Titanium Alloy

Nb–Ti alloy superconductors have been the "workhorse" materials of the superconductor industry for the past 40 years [1]. They were discovered in the 1960s to have a high upper critical field ($\sim$11 T at 4.2 K and 14 T at 2 K), to codraw well with Cu and to have good ductility. Early magnets performed poorly due to premature quenching, which was not understood at the time. However, the importance of subdividing the superconductor in order to provide

intrinsic stability against flux jumps was recognized in the late 1960s [16]. This discovery, together with the discovery by the Rutherford group [34] that twisting the wire would reduce filament coupling, led to wires with greatly improved properties. Several major milestones were achieved in the 1980s using Nb–Ti, including the first superconducting accelerator, the Tevatron, in 1983, and the first large-scale superconducting commercial application, MRI, in the early 1980s.

The properties of Nb–Ti alloy superconductors improved slowly throughout the 1960s and early 1970s, so that by the time conductor was ordered for the Tevatron, a critical current specification of 1800 A/mm^2 (5 T, 4.2 K) could be achieved. Although a recipe for improving J_c had been developed along empirical lines by industrial manufacturers, the technology lacked a good fundamental understanding. In the early 1980s, a collaboration of university, national laboratory and industrial partners, led by the University of Wisconsin Applied Superconductivity Center, was formed to improve the understanding of flux pinning in Nb–Ti and to incorporate this improved understanding into the manufacturing technology for Nb–Ti [35]. The driving force at the time was the high performance requirements for the Superconducting Super Collider, and much of the work was sponsored by the Office of High Energy Physics of the U.S. Department of Energy (DOE). The steps taken to improve Nb–Ti performance can be divided into two categories—extrinsic and intrinsic, and an apt description of the process of systematic improvement, coined at one of the LTS workshops, is "peeling the onion."

First, several extrinsic limitations were discovered and corrected. These include the formation of intermetallics at the Cu/Nb–Ti interface during the precipitation heat treatment steps [36]. This was corrected by the use of a Nb diffusion barrier wrapped around the Nb–Ti filaments during billet construction [37]. Another problem is the tendency of the filaments to undergo distortion during fabrication, called "sausaging." Sausaging is caused by the difference in mechanical properties between the Nb–Ti and Cu matrix, and can be prevented by placing the filaments in a dense stack in the Cu matrix, rather than having them widely spaced [38]. Adjusting the placement and temperature of the multiple heat treatments required to achieve a high J_c can also help reduce the differences in mechanical properties between the Nb–Ti filaments and the Cu matrix.

The first intrinsic limitation that was found and corrected was the inhomogeneity of the Nb–Ti alloy, caused by a distribution of Ti-rich regions [39]. These responded very differently to the precipitation heat treatment and, thus, prevented establishing an optimum heat treatment to yield a uniform and predictable distribution of alpha-Ti precipitates necessary for effective flux pinning [40]. As a result of the improved understanding of Nb–Ti alloys, the current density was increased by about 100%, to $>$3700 A/mm^2 at 5 T, 4.2 K [41].

Multifilamentary Nb–Ti fabricated by conventional technology is a mature field, and the rapid improvements seen from 1983 to 1990 have slowed. However, a new approach to

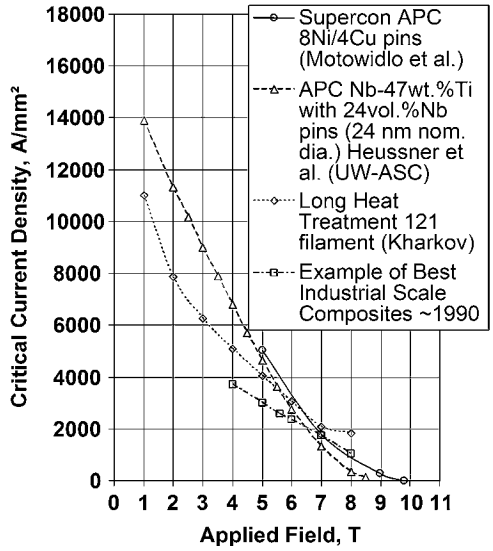

Fig. 4. Critical current density of conventional and artificial pinning center composites, showing that it is possible to further enhance the current density of Nb–Ti by tuning the pinning center properties. Data is sourced from [41], [43], and [45].

the fabrication of Nb–Ti using "artificial" or engineered pinning centers (APCs) was suggested in 1985 and continues to enable progress [42], [43]. The basic idea is to incorporate a normal metal into the Nb–Ti at the beginning of the fabrication process and then to coreduce both Nb–Ti and the pinning center material by extrusion and drawing until the normal metal component has the correct size and spacing for optimum vortex pinning. The original approach was to drill holes in a Nb–Ti ingot and load metal rods that are compatible with the Nb–Ti (e.g., Nb). However, a more practical method from the manufacturing standpoint is to assemble a jellyroll of alternating Nb–Ti and Nb sheets. This jellyroll is loaded into a Cu can, compacted, and extruded to produce a "clad monofilament" element, which is cut into short lengths, loaded into the final Cu can, and extruded. The resulting multifilamentary composite is then drawn to final wire size. Using this approach, long lengths of Nb–Ti superconductor have been produced with J_c values exceeding those obtained for conventionally processed Nb–Ti, in the field range from 2–7 T. Initially, the high field (6–8 T) performance was not as good for the APC wires; however, recent results with ferromagnetic pinning centers in place of the Nb pinning centers have shown excellent properties at higher fields as well [43], [44]. The best J_c values for both conventional and APC Nb–Ti are shown in Fig. 4. In this graph, we also show some recent optimization using very long heat treatment times by the Khar'kov group that have driven the Nb–Ti critical current density to over 4000 A/mm^2 at 5 T, 4.2 K [45].

The present rate of production for Nb–Ti superconductor is over 200 tons/year, with one project, the Large Hadron Collider (LHC) of Consel European pour la Recherche Nucleaire (CERN), accounting for about half of the total. The LHC superconductor procurement will be complete in 2006. It is unlikely that the growth rate of MRI systems will be adequate to make up for this lost LHC volume, and the next large international fusion magnet project, International

Tokomak Experimental Reactor (ITER), will utilize mostly Nb_3Sn. However, much of the existing Nb–Ti production capacity and equipment will very likely be needed for the ITER Nb_3Sn procurements (see below). Thus, while the LTS industry is expected to undergo a transition, overall production volume is expected to remain steady.

V. Niobium–Tin

Nb_3Sn in a prototype wire form was the first material to show the possibility of high-field superconductivity in 1961; its H_{c2} reaches $\sim$30 T at 2 K, substantially exceeding Nb–Ti and making it the prime candidate for higher magnetic field systems [1]. Progress was initially limited, primarily due to the fact that Nb_3Sn is a brittle intermetallic compound which could only be made as a tape, while Nb–Ti is a ductile alloy, enabling very flexible architectures. However, starting in the early 1970s, practical Nb_3Sn multifilamentary conductors were successfully developed with the bronze route and many laboratory and high field NMR magnets were and are still being made. As applications moved to fields exceeding the practical operating field of Nb–Ti (about 9 T at 4.2 K and 12 T at 1.8 K), there was strong interest in Nb_3Sn, driven also by plasma containment applications.

There are several processes for fabricating multifilamentary Nb_3Sn wires that permit processing ductile precursors down to final wire size, followed by reaction of the components to form the Nb_3Sn intermetallic compound. The so-called bronze process involves codrawing Nb rods in a matrix of Cu–Sn alloy, which is made as Sn-rich as practical, while still maintaining good ductility (around 15 wt% Sn). However, much residual Cu is left behind after reaction, making A_{sc} a small (~ 0.2) fraction of the conductor package. To obtain a higher volume fraction of Nb_3Sn and, hence, higher overall J_c values, the internal Sn process was introduced. This multifilamentary composite contains Nb filaments in a Cu matrix and the Sn is introduced as a separate component, usually as a core added to the Nb–Cu multifilamentary composite. These two processes, together with the newer powder-in-tube (PIT) process, are illustrated in Fig. 5.

Recently, the two principal technology drivers for Nb_3Sn have been magnets for high-energy physics (HEP) accelerators and for magnetic fusion energy (MFE); a third, though less publicly discussed one, has been very high field NMR magnets used for the 800- and 900-MHz class spectrometers. In the early 1990s, both HEP and MFE initiated programs to develop superconductors and magnets for high field ($>$12 T) applications. The focus of the HEP effort was dipole and quadrupole magnets, while the fusion program focus was solenoidal and toroidal field coils for ITER [46]. Both programs chose Nb_3Sn as the most promising conductor for high fields, and conductor development programs were initiated in industry. During the 1990s, the ITER program was the primary customer for Nb_3Sn, ordering more than 20 tons of wire from companies in Europe, Japan, Russia, and the United States. This program helped establish a large-scale

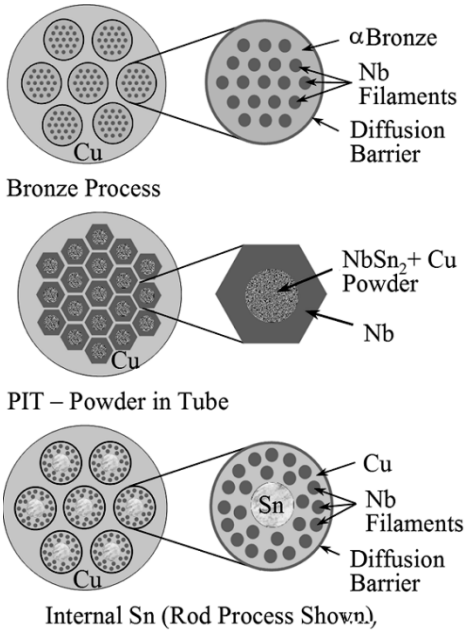

Fig. 5. Bronze, PIT, and internal Sn conductor processes for fabricating Nb_3Sn. (Figure courtesy of M. Naus, University of Wisconsin, Madison).

production capability for Nb_3Sn, and stimulated further development of bronze, internal Sn, and PIT multifilamentary wire fabrication techniques [47], [48].

As a result of the accelerator dipole design efforts at the U.S. high energy physics laboratories, it became clear that higher field, cost-effective magnets required higher current density and reduced manufacturing costs. Thus, in 1999, DOE initiated a new conductor development program for Nb_3Sn [49], with the goal of providing a cost-effective, high-performance superconductor for next-generation high energy physics colliders, as well as upgrades for existing colliders at Fermi National Accelerator Laboratory, Batavia, IL, and CERN. The target conductor specifications are listed in Table 1. The emphasis is on Nb_3Sn made by industrial partners with large-scale Nb_3Sn production experience. Improvements in the critical current density J_c in the noncopper part of the wire has been the highest priority, followed by reduction in the effective filament diameter d_{eff}, and then by lower cost.

The first-priority goal of the program, achieving an increase in the noncopper J_c (12 T) from 2000 to 3000 A/mm^2, was reached in 2002 [50]. This goal was achieved without an increase in cost per kilogram, so the cost-performance ratio has decreased significantly (Fig. 6). This new wire not only has excellent J_c values, but can be produced in long lengths as well. In 2003, Oxford Superconducting Technology delivered 100 kg of this wire for use in a new dipole magnet at Lawrence Berkeley National Laboratory (LBNL), Berkeley, CA, that recently reached a new dipole field record of nearly 16 T [51].

Development of magnet designs that maintain a relatively low transverse stress on the conductor in the highest field regions, coupled with improvements in Nb_3Sn J_c values,

Table 1
Target Specifications for HEP Conductor

J_c (non-copper, 12T): 3000 A/mm^2
J_e (12T): >1000 A/mm^2
Effective filament size: <40 μm
Process unit size: scaleable to >100 kg and average piece lengths >10,000 m in wire diameters of 0.3mm to 1.0 mm
Wire cost: <$1.50/kA-m (12T, 4.2K)
Short heat treatment times: maximum 400 hrs; target 50 hrs for wind and react magnets

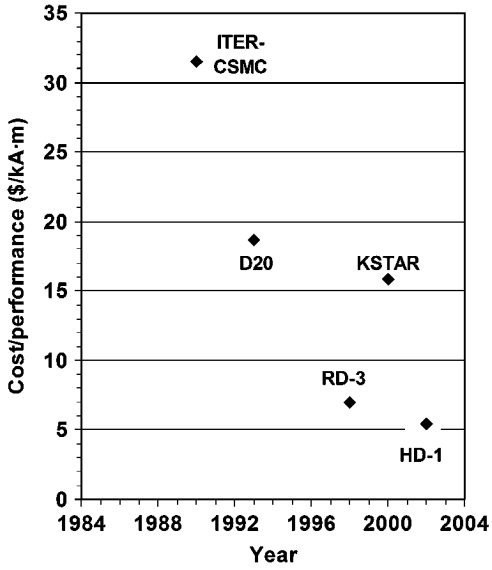

Fig. 6. Cost/performance parameters for filamentary Nb_3Sn conductors used for tokamak plasma containment devices (ITER and KSTAR) and for high-field accelerator dipoles (D-20, RD-3, and HD-1). The trends show that cost has come down markedly with time, partly because of production experience and partly because J_c has markedly increased. J_c (12 T, 4.2 K) of conductor for HD-1 is about four times that for ITER.

means that Nb_3Sn has the technical performance and cost-effectiveness for use in dipole magnets up to at least 16 T, and perhaps up to 18 or 20 T. Detailed magnet design efforts are underway at several HEP laboratories to determine how far Nb_3Sn can be pushed, and for the selection of the best conductor design for such fields.

After completion of the first phase of ITER, that project is moving ahead with the next phase, which is an international tokamak test facility [46]. The ITER design requires the production of an enormous quantity of Nb_3Sn conductor (approximately 500 t over 3–4 years). The main challenge will be to scale up the yearly production level from the present 10 t/manufacturer to the required 150 t/manufacturer.

The largest present commercial application of Nb_3Sn is in the area of NMR magnets. This application is growing rapidly and moving steadily to higher fields. Recent improvements in J_e of Nb_3Sn have extended its useful field range to at least 21 T at 1.8 K, making persistent mode 900-MHz systems possible. Significant challenges had to be overcome in order to achieve these high fields in a practical NMR magnet. Since this is a very competitive commercial area, magnet construction details are not usually published. Oxford/Varian and Bruker both have working 900-MHz systems with an operating field of 21.1 T and very low field drift rates. The increased performance of recent Nb_3Sn conductors for HEP use at 10–16 T has also benefited very high field applications, because the upper critical field was increased [52]. It is now widely expected that the newer Nb_3Sn conductors will permit 1-GHz NMR magnets to be made of Nb–Ti and Nb_3Sn. This would require persistent operation at a field of about 23.8 T in a material with an upper critical field of about 28–29 T at the operating temperature, a truly challenging but attainable goal.

VI. Niobium–Aluminum

The driver for interest in another A-15 compound Nb_3Al is an even higher magnetic field capability than Nb_3Sn. Two approaches for fabricating Nb_3Al are being developed. The first is analogous to the internal tin process for fabricating Nb_3Sn. A composite of Nb and Al is formed, most often using a jelly roll technique to make the composite subelement which is extruded. This step is followed by drawing, hexing, and restacking into the final composite with a Cu matrix, which is then drawn to final size and reacted to form Nb_3Al. Sumitomo Electric Industries, Osaka, Japan, has used this approach to manufacture several tons of wire for a model coil for the ITER project; so manufacturability has been demonstrated [53]. However, the Nb_3Al layer formed by this diffusion step is off-stoichiometry, and both T_c and H_{c2} are suppressed. This in turn leads to a J_c versus field performance inferior to Nb_3Sn.

An alternate processing route has been developed by the former National Research Institute for Metals (NRIM), now the National Institute for Materials Science (NIMS) Tsukuba, Japan, in Japan. In this process, a composite of Nb and Al is assembled and drawn to produce a fine-scale composite where the Nb and Al components have 100–200-nm dimensions. This composite is heated rapidly to 1900 °C and then quenched to produce a body-centered cubic solid solution alloy with the stoichiometric Nb_3Al composition. Finally, the composite is heated to about 800 °C, where the A15 phase is formed, with high T_c, H_{c2}, and good

high-field J_c characteristics. By 1996, the NRIM team scaled up the rapid heat/quench step to produce relatively long lengths using a reel-to-reel system where the wire was resistively heated and then quenched in liquid Ga [54]. Ongoing optimization of this process has steadily raised T_c, J_c, and H_{c2} of rapidly quenched Nb_3Al [54], [55]. However, manufacture of the precursor remains challenging, as does the production quenching, addition of stabilization, and achieving properties superior to the most recent Nb_3Sn. The NIMS group remains very active in pursuing the possibilities of the rapid quench technique and have seeded additional studies on this important material [56].

Chevrel phases, with intermediate transition temperatures, were also actively developed for superconducting wire [1], but this effort has now been largely abandoned.

VII. BSCCO-2212

The HTS BSCCO-2212, with a T_c of around 90 K, has been eclipsed for most high-temperature applications by BSCCO-2223, which has a higher T_c and a higher irreversibility field (see next section). However, BSCCO-2212 has superior J_c at low temperatures (below about 20 K) and high fields. For example, using their preannealing intermediate rolling (PAIR) process on long length dip-coated tapes, Showa Electric Wire and Cable Co. Ltd., Kawasaki, Japan, in collaboration with NRIM (NIMS) and the Japan Science and Technology Corporation, Tokyo, Japan, have achieved J_c of 7100 A/mm^2 in self-field and 3500 A/mm^2 in 10 T parallel to the tape plane [56]. This has enabled application in high-field inserts for NMR and other applications [57], [58]. At present, BSCCO-2212 holds the record for producing the highest field with a superconducting magnet. The BSCCO-2212 tape, produced by Oxford Superconducting Technology (OST), Carteret, NJ, and wound into an insert magnet at the U.S. National High Magnetic Field Laboratory (NHMFL), Tallahassee, FL, achieved a 5-T increase in field in a background field of 20 T from a copper Bitter coil [8].

Also, BSCCO-2212 has been fabricated as a round wire in a silver matrix [Fig. 1(c)] with excellent critical current—J_e at 20 T, 4.2 K over 500 A/mm^2 [59]. This wire can be used as a direct substitute for LTS wires in Rutherford-type cables [60] in applications such as accelerator magnets, and the first series of prototype coils have been made [61]. Two issues must be resolved for this application to proceed. First, the cost/performance ratio must be reduced from the roughly \$50/kAm value at present, to under \$10/kAm. Second, practical methods for achieving stringent heat treatment control in an industrial environment must be developed. A partial melting step is required to achieve optimum properties, and the temperature must be controlled to within a few degrees at around 870 °C. At present, three companies worldwide are manufacturing BSCCO-2212—Showa, Nexans, and OST. All companies have demonstrated excellent J_c values. Showa and Nexans, Jeumont, France, [62] have both demonstrated that they can make 1600–m lengths of wire without breakage and can control the heat treatment to achieve uniform properties.

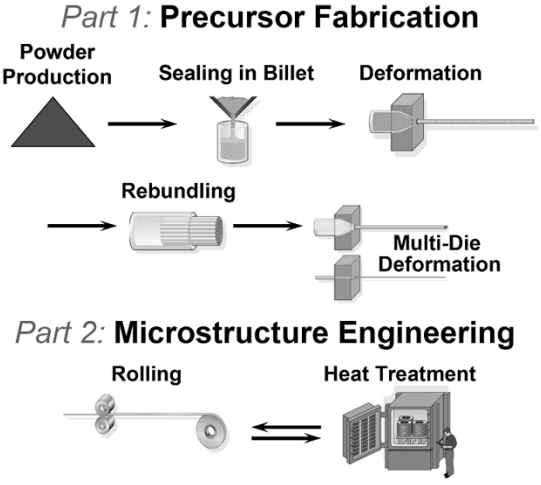

Fig. 7. Schematic of the OPIT process for making Bi-2223 superconducting wire such as that shown in Fig. 1(d). Starting powder based on Bi-2212 and required Ca–Cu–O balancing ingredients is packed in a silver billet, deformed to a monofilament stack and then rebundled into a multifilament stack. The heat treatment which drives the 2212 to 2223 phase conversion occurs in two or more heat treatments separated by an intermediate rolling step which helps densify the tape.

VIII. BSCCO-2223

The HTS $(Bi,Pb)_2Sr_2Ca_2Cu_3O_{10}$, called BSCCO-2223, with a T_c of about 110 K, is used in the first generation of commercial HTS conductor, a composite of the superconductor with silver [3]. As shown in the cross section in Fig. 1, this first-generation HTS wire has a tape shape, typically 0.2 by 4 mm, consisting of 55 or more tape-shaped filaments, each 10 μm thick and up to 200 μm wide, embedded in a silver alloy matrix. The filaments consist of grains of BSCCO-2223, up to 20 μm long, often arranged in colonies sharing a common c axis. For some applications, the wire is laminated to stainless steel tapes on either side for enhanced mechanical properties and environmental protection. This kind of HTS wire is manufactured by a number of companies, including American Superconductor Corporation (Devens, MA), European Advanced Superconductor GmbH (formerly Vacuumschmelze, Hanau, Germany), Innova Superconductor Technology (Beijing, China), Sumitomo Electric Industries Ltd. (Japan), and Trithor GmbH (Rheinbach, Germany). Worldwide capacity exceeds 1000 km per year.

While precise details of the industrial production process are not public, the basic PIT deformation process is schematized in Fig. 7 [3], [10]. A powder consisting of a mixture of Pb-containing BSCCO-2212, alkaline earth cuprates, copper oxide, and other oxides is initially prepared by an aerosol, spray-dry or simple oxide mixing process; the overall cation stoichiometry is chosen to match that of BSCCO-2223. The powder is packed into a silver tube, which is sealed, evacuated, and drawn through a series of dies, elongating it into a hexagonal rod. These rods are next cut, assembled into a multifilament bundle (55–85 filaments are typical), and inserted into a second silver or silver alloy tube. This tube is sealed, evacuated, and further drawn into a fine round wire,

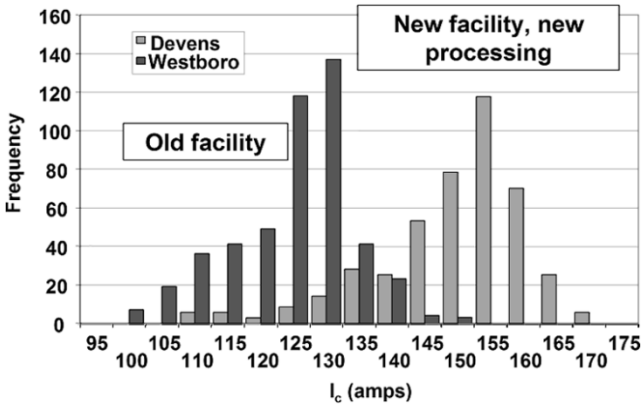

Fig. 8. The I_c (77 K, self-field) distribution from production runs of recent AMSC unlaminated first-generation HTS wires based on BSCCO-2223, with 4.2×0.21 mm^2 cross section and >150 m length (courtesy of AMSC). The 170-A result corresponds to an engineering critical current density of over 190 A/mm^2.

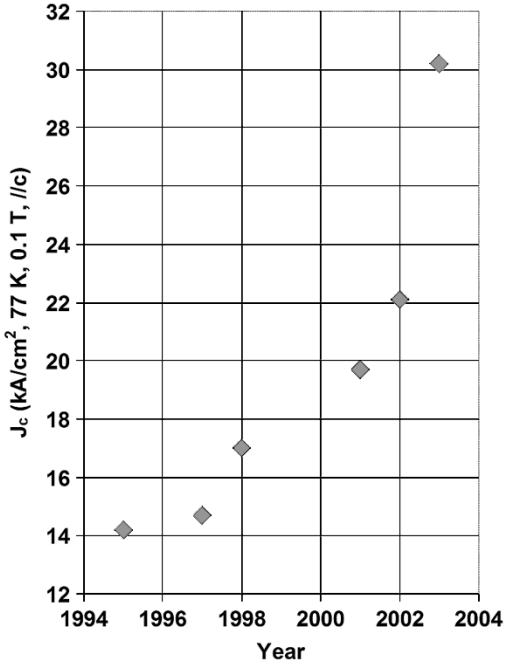

Fig. 9. Steady progress in understanding the current limiting mechanisms in BSCCO-2223 first-generation HTS wires has led to continued progress in raising the current density expressed at the benchmark field of 0.1 T at 77 K, at which field the tapes are always fully penetrated by the external field and self-field suppression of the J_c is negligible. The highest value sample plotted above has a strongly self-field limited critical current of 182 A (77 K) in zero-applied field, while its estimated self-field-free I_c is 235 A, corresponding to J_c of 266 A/mm^2. (Courtesy of AMSC and the University of Wisconsin, Madison.)

which is subsequently deformed to a tape shape in a rolling mill, in multiple steps of rolling and heat treatment to texture and react the powder inside the wire to form BSCCO-2223. The superconducting fill factor is typically 30%–40%.

Three important insights into this process are as follows. First, the use of silver, a relatively expensive metal, is necessary because silver, like other noble metals, is inert to the superconductor, and particularly because it permits rapid oxygen diffusion at high temperatures without itself oxidizing. This latter property allows control of the oxygen activity in the reaction of the powder to BSCCO-2223. The silver also acts as an electrical and mechanical stabilizer in intimate contact with the superconducting filaments. Second, the use of the rolling process to flatten the wire to a tape shape is necessitated by the need to texture the powder, which consists of mica-like grains of BSCCO-2212, along with the less aspected other oxides. High texture is the key to a high current density in the final product. Third, the success of this process with BSCCO rather than other HTS materials appears to be related to easy slip along the weakly bonded double-Bi,Pb-oxide layers; this facilitates texturing during the rolling deformation. The easy slip plane also enables formation of colonies or stacks of many highly aspected grains rotated in apparently random orientations with respect to each other around a common c axis perpendicular to the CuO planes. This structure is believed to facilitate current flow as discussed in Section III above [27].

J_c of BSCCO-2223-based wire has been a research and development focus worldwide for 15 years, increasing steadily over time, with long-length (>150 m) wires now achieving up to a maximum of 170 A and an average above 150 A in end-to-end I_c at 77 K and self-field in 0.21×4.2 mm tape (Fig. 8) [3], [10]. The maximum I_c corresponds to an engineering critical current density of close to 180 A/mm^2. Given a 40% superconductor fill factor in the wire, this corresponds to J_c of 450 A/mm^2. At a temperature of 30 K and 2 T, of interest, for example, in rotating machinery applications, the current density is enhanced over its 77 K self-field value by almost a factor of two. These performance levels have been applied successfully in a variety of commercial-level prototypes and appear adequate for most power applications. At this point, the main value of further increasing I_c is reducing the price–performance ratio \$/kAm. First-generation HTS wires are currently sold at \$150–200/kAm, and with further manufacturing efficiencies, price–performance of \$50/kAm is expected, even without further increase in I_c.

More progress in I_c seems feasible, based on an improved understanding of the materials science of BSCCO-2223 and its phase conversion, closely correlated to knowledge of where the current flows and how it is limited by microstructural defects [63]. This task has been pursued by the DOE-supported Wire Development Group, an industry-national lab-university partnership, during the past dozen years. Recently there has been progress in mitigating two important current-limiting mechanisms. One is residual porosity left over from the dedensification that occurs during the reaction of 2212 phase to 2223 and the cracking that occurs during the intermediate rolling step that is required to remove such porosity. The second is due to unreacted streaks of 2212 phase that occur either as intergrowths within the 2223 phase or as individual grains within a larger colony of $\sim$10 2223 grains which share a common c axis. Porosity and cracking have been remarkably reduced by processing at hydrostatic pressures of up to 150 bar, [63]–[66] advancing J_c at the appropriate benchmark of 0.1 T at 77 K to 304 A/mm^2, as shown in Fig. 9. The corresponding zero-field value at

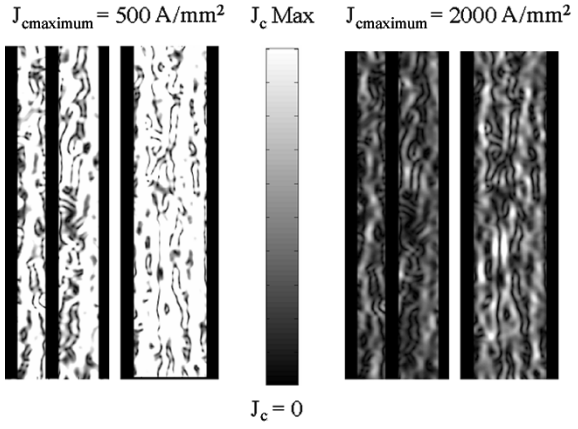

Fig. 10. Current distribution reconstructions from magnetooptical images at 77 K and 40-mT field parallel to the ab planes of two monofilament AMSC BSCCO-2223 first-generation HTS wires. This imaging condition develops a current density that is within 5% of the self-field current density under normal self-field test conditions. The J_c (77 K, self-field) values for the 1 atm-processed tape was 390 A/mm^2 and that for the 148 bar-processed (overpressure-OP) tape (right-hand pair) was 480 A/mm^2. In the left-hand pair, the brightest areas are 500 A/mm^2 but 2000 A/mm^2 in the right pair. The many bright areas in the right-hand picture show that many regions exceed 2000 A/mm^2. (The black bar in the 1 atm-processed tape is a nonmeasurable area in the magnetooptical image.) Data taken from [63].

77 K has surpassed 200 A in a 4.2×0.21 mm^2 wire. This marks a doubling of J_c in the last five years, and the pace is accelerating as fundamental understanding grows. Similarly, improved heat treatments have reduced the amount of residual 2212 phase. Recent magnetooptical current reconstructions (Fig. 10) on a high-J_c monofilament conductor with $J_c\ (77\ \mathrm{K}, \mathrm{sf}) = 350$ A/mm^2 [63] show that there is still great headroom in the system. Remarkably, J_c locally reaches well over 2500 A/mm^2, five times higher than its average value, and regions of J_c exceeding 1000 A/mm^2 are 50 to 100 μm long, several times the $\sim$20 μm grain length. Although there is a tendency for the highest J_c regions to be located at the Ag–superconductor interface, in fact, very high J_c regions are located throughout the filament. The J_c distribution is both higher and spatially larger in the overpressure processed tapes, consistent with strong reduction of porosity and cracking.

With the strong performance improvement, cost reduction, and successful manufacturing scale-up, first-generation BSCCO-2223-based HTS wire has proven successful in meeting applications requirements and is being widely used in commercial-level prototypes. No other HTS wire technology is likely to replace it for at least several years [10]. It will be the basis of the first commercial HTS applications, which are expected to be largely in the electric power arena and in magnets where operation at temperatures above 30 K is preferred. The longer term future for this wire depends on the degree to which its price–performance ratio can be reduced and on the success of alternatives like second-generation HTS wire based on YBCO-coated conductor.

IX. YBCO-Coated Conductors

The vision for a second generation of HTS wire is based on a quasi-single-crystal layer of $YBa_2Cu_3O_7$, with grain-to-grain misorientations of order 5° or less to enable high current by exploiting the strong grain-to-grain coupling which occurs under these conditions (see Section III) [9], [67]–[74]. Such a continuous YBCO film must be manufactured over long lengths and at low cost with only a nominal Ag fraction [75]. After about a decade of effort, it was shown in 2003 by multiple fabrication routes that continuous processing of lengths of 10–50 m with high critical current properties is possible, opening the path to production scale up. Coated conductors use thin-film technology to apply an epitaxial superconductor layer to a highly biaxially textured tape-shaped template, whose texture the YBCO replicates. This is a complex, metal-supported, multifunctional, multilayer oxide structure. Cost models for coated conductors, particularly those made by nonvacuum methods, predict values below \$10/kAm (77 K, 0 T); well below the effective price–performance of copper [75]. Because of the significantly higher irreversibility field of YBCO compared to BSCCO (Fig. 2), second-generation HTS wire also offers the opportunity to achieve higher temperature operation in a given magnetic field.

All coated conductors include a flexible substrate, preferably of strong and nonmagnetic or weakly magnetic metal, typically $\sim$50 μm thick, on top of which is a multifunctional oxide barrier or buffer layer, typically less than $\sim$0.5 μm thick, on top of which is the superconducting YBCO layer 1–3 μm thick. A protective Ag layer of a few micrometers and a thicker Cu protection and stabilization layer complete the conductor [76]. The textured template is created by one of two basic methods, either by texturing the buffer layer by ion beam assisted deposition (IBAD) [67]–[71], [77], or inclined substrate deposition (ISD) [78], [79], or by deformation texturing the metal substrate with the rolling assisted biaxially textured substrate approach [72]–[74] and applying epitaxial oxide buffer layers (trademarked RABiTS by Oak Ridge National Laboratory, Oak Ridge, TN).

The IBAD method [67] allows for the use of strong, nonmagnetic Ni-superalloy or stainless steel substrates on which a textured IBAD layer of aligned yttria-stabilized zirconia (YSZ), gadolinium zirconate (GZO), or magnesium oxide MgO can be deposited [70], [77]. This process can achieve good texture (full-width at half-maximum (FWHM) $\sim 10^\circ$) with a layer of YSZ that is $\sim$0.5–1 μm thick. However, deposition of IBAD-YSZ is widely considered to be too slow, and, thus, too expensive, to be commercial. IBAD-MgO, however, produces excellent texture within the first 1–2 nm, and, thus, deposition may be rapid enough to be commercially cost-effective [70], [77]. The X-ray pole-figure FWHM of recent IBAD-MgO coated conductors is much better than for IBAD-YSZ, being of order 2–4° and, thus, genuinely approaching single crystal structure for the YBCO overlayer [70], although performance so far does not fully reflect this unusually high degree of texture, and achieving the required atomic level surface roughness over long lengths has proven

challenging. The inclined substrate deposition (ISD) process is more rapid than YSZ-IBAD, since there is no resputtering during deposition, but in work to date, the texture is not as high [78], [79]. ISD may also permit simpler buffer structures. Other ion texturing processes for buffer layer deposition have also been explored [80]. All these methods of producing a textured buffer layer rely on physical vapor deposition processes, whose cost is an obstacle to achieving price–performance competitive with copper.

An advantage of the RABiTS approach is that texture can be achieved with a low-cost nonvacuum process. A strong [100] cube texture is introduced into the substrate by conventional rolling and recrystallization. Although the RABiTS approach was developed initially with pure nickel [72], substrate materials with more robust mechanical properties and reduced magnetism, notably nickel with 5 atomic % tungsten, have now replaced pure Ni and achieved FWHM below 5° [73].

The buffer layer is also in active development. At present, virtually all processes employ a multifunctional buffer in which the functions of seed layer for the metal-oxide interface, a metal and oxygen diffusion barrier, and cap layer lattice-matching to the YBCO interface are separated. Many such architectures are presently vying for selection. Seed layers of Y_2O_3, Gd_2O_3, or NiO have all been employed. YSZ is by far the most common Ni diffusion barrier or buffer, while CeO_2 is generally employed for the cap layer interface to YBCO. IBAD–MgO buffer layers are also in rapid development.

Many different deposition methods for the crucial epitaxial YBCO layer have been developed, all achieving high critical currents in short samples. Thus, the choice among them can be driven by low cost. The leading low-cost alternatives are those based on liquid-phase chemical routes using metal–organic deposition (MOD) [75], [76] or on metal–organic–chemical vapor deposition (MOCVD) [81], though advocates of fast electron-beam deposition of either metal constituents or the so-called BaF_2 route remain, as do the advocates of so-called fast pulsed laser deposition. It is also becoming increasingly recognized that the use of higher T_c versions of the YBCO structure, for example, $RBa_2Cu_3O_7$, where R might be Eu or Nd with a T_c of 94–95 K could offer significant benefit to 77 K properties.

The design of a coated conductor is such that about 50-μm substrate thickness is needed to support 1–5 μm of YBCO, giving a superconductor fraction which is at best 5%–10% of the cross section, as compared to 30%–40% in the first-generation HTS wire of Fig. 1. Present short samples of both IBAD and RABiTS conductors can both exceed 2 MA/cm^2 at 77 K for YBCO layers up to $\sim$2 μm, enabling currents of 400 A/cm width or 160 A in a 4-mm-wide tape, which is comparable to first-generation wire. A significant and not well understood obstacle to further increasing I_c is that in many cases J_c of the YBCO layer degrades with increasing thickness. Loss of epitaxy, increasing porosity, a microstructural transition through thickness, and possibly a two-dimensional to three-dimensional transition of the vortex structure

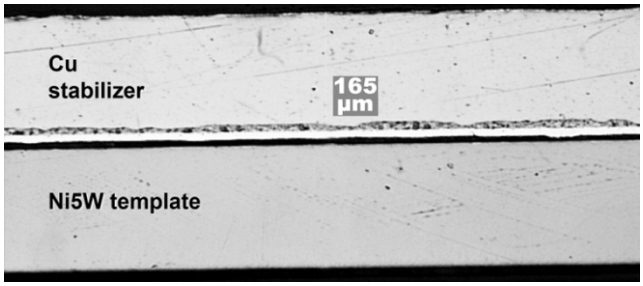

Fig. 11. Illustrative architectures [76] of a neutral axis YBCO coated conductor, showing the copper stabilizer, the solder joining the Cu to the YBCO, and the Ni$_5$ at %W textured template. (Courtesy of AMSC.)

once the layer gets thicker than about $\sim$0.5 μm may all play significant roles [82].

Progress on continuous reel-to-reel processes for making coated conductors has been particularly rapid in the recent year. Continuous 10–100-m lengths of 1-cm-wide conductor with end-to-end critical currents as high as 270 A/cm width A at self-field at 77 K show that this multistep fabrication process is being mastered [83]. Uniformity along the length indicates that kilometer-length wires should be possible. Lamination of hardened copper strip to the multilayer of metal substrate, buffer, YBCO, and Ag passivation is an important step to achieve a robust, stabilized conductor. In particular, conductor designs such as those shown in Fig. 11 include a "neutral axis" conductor in which the YBCO lies at the position of zero tensile or compressive strain during bending, or a "face-to-face" conductor in which two layers of YBCO, coupled through an internal stabilizing copper layer, provide alternative current paths for each other in case of a defect in one [76].

No fundamental technical barriers to the fabrication of long-length coated conductors appear to exist, although much work remains to scale up the process to long lengths. Work will also need to focus on improving flux pinning in YBCO so as to achieve higher J_c in field and a monotonic J_c as a function of field angle. The introduction of these second-generation HTS wires into practical applications will be facilitated by designing them with similar size and rating as first-generation HTS wires, since all present electrical equipment design is being done with first-generation wires. Second-generation wires are also very attractive for current limiting applications because of the high electric fields that can be reached when the superconductor goes normal in response to a high fault current.

In short, second-generation HTS wires show promise for achieving a price–performance ratio below that of copper and for providing new performance features, thus significantly expanding the HTS market. Expected applications are largely in the electric power arena and for magnets where operation at temperatures above 30 K is preferred. Active research and development is underway at Los Alamos, Oak Ridge, and Argonne National Laboratories, at the International Superconductivity Technology Center (ISTEC), Tokyo, Japan, and at a variety of European laboratories and universities. Industrial programs are underway at American

Superconductor Corporation and the Intermagnetics General subsidiary SuperPower Inc., Latham, NY, at Fujikura Ltd., Tokyo, Japan, Furukawa Electric Co. Ltd., Tokyo, Japan, and Sumitomo Electric Industries Ltd. in Japan, and at Theva GmbH in Europe. However, it should be emphasized that it will take several years to achieve a meaningful scale-up to long lengths and adequate production capacity for the commercial market.

X. Magnesium Diboride

In early 2001, the Akimitsu group in Japan discovered that the long-ago-synthesized compound magnesium diboride MgB_2 was a hitherto unappreciated 40 K superconductor [84]. Extensive work on MgB_2 has now shown that it is a "conventional" s-wave superconductor but with the unconventional property that it contains two, only very weakly coupled superconducting gaps. This two-gap property is very important to its high-field performance potential [85]–[87].

A key early discovery was that randomly oriented grain boundaries in MgB_2 are not obstacles to current flow, in spite of the fact that its alternating Mg and B sheet structure makes it electronically anisotropic [88]. The magnitude of this H_{c2} anisotropy is under intense study at present. In single crystals, this anisotropy is quite strongly temperature dependent and increases with decreasing temperature to values of five to seven [89]. In a "clean," very low H_{c2} limit, the zero-temperature perpendicular upper critical field $H_{c2}^{\perp}(0)$ is only 3–4 T, while the equivalent parallel field value, $H_{c2}^{\parallel}(0)$ reaches ~15–17 T. Study of dirty-limit films shows that $H_{c2}^{\perp}(0)$ can reach more than 40 T, while $H_{c2}^{\parallel}(0)$ exceeds present measurement fields and probably is exceeds 70 T [90]. An important conclusion is that the $H_{c2}(T)$ envelope of MgB_2 can exceed that of Nb_3Sn at any temperature, even in the weaker condition of field perpendicular to the B sheets. Because grain boundaries appear to carry current independent of misorientation, round wire conductors without texture are practical, provided the limitation of the anisotropic H_{c2} is accepted. As noted above, this anisotropy actually decreases as H_{c2} is enhanced, primarily because the lower perpendicular H_{c2} increases more rapidly than the parallel value.

MgB_2 can be made by the PIT process and many groups have made prototype wires, using both prereacted (*ex situ*) MgB_2 powder and mixtures of Mg and B powders, which must be reacted to MgB_2 *in situ* within the wire [12]. A particularly rapid use of MgB_2 wire has been for low thermal conductivity current leads in the ASTRA-2 satellite [91]. However, it is clear from analyses of the electrical resistivity of many samples, including wires, that bulk MgB_2 is actually very far from being fully sintered or electrically connected [33]. Porosity and wetting by B and perhaps oxygen-rich phases obstruct many grain boundaries [92], [93] and porosity is still endemic in wires [12]. Yet even so, J_c exceeds 10^3 A/mm^2 at lower temperatures and fields. In well-connected thin films J_c values as high as 10^5 A/mm^2 have been reported [94]. It, thus, appears clear that at least in the temperature range below about 25 K, there is neither a current density, nor an upper critical field barrier to the application of MgB_2. Thus, MgB_2 wires could become a credible competitor to LTS-based wires or to BSCCO-based wires used in low-temperature (<25 K) applications. An additional quality is that the H_{c2} transition appears to be rather sharp, much more similar to low-T_c materials [95] than to HTS materials [96]. Thus, high n values and even persistent mode magnets appear feasible, making MgB_2 a potential NMR or MRI magnet conductor.

Another advantage of MgB_2 is that the raw material costs of both B and Mg are low; reasonable estimates suggest that even for appropriately purified material, they will be several times less than those of Nb-based superconductors [97]. Thus, the principal uncertainties of the technology are the costs and difficulties of developing the PIT composite technology or some alternative. By way of comparison, PIT technology is employed for Nb_3Sn manufacture using powders of $NbSn_2$ inside Nb tubes. Present manufacturing costs of Nb_3Sn conductors using PIT processes are about five to six times higher than conventional metal-working approaches to Nb_3Sn composites. Some of this is due to the costs of making appropriate starting powders but a large part is also due to the small scale on which PIT–Nb_3Sn is presently made. It is worth noting that the quality and J_c of PIT-Nb_3Sn composites made by ShapeMetal Innovation, Enschede, The Netherlands, are very high—conductors containing two hundred to five hundred 15–25-μm-diameter filaments have been made in magnet lengths [52]. Such filaments are completely decoupled, which is not at all true of the filaments in either BSCCO-2212 or -2223 multifilamentary conductors. If MgB_2 is to challenge LTS, the goal must be to replicate this quality, while keeping production costs down.

In summary, MgB_2 is a most intriguing new entry into the superconductor wire arena. By making MgB_2 dirty, just as was done earlier when Ti was added to Nb_3Sn, H_{c2} can be greatly enhanced [86], [87], [90], [98], [99]. Indeed the two-gap nature of MgB_2 adds additional versatility to the material, because the low temperature value of H_{c2} is determined by the electronic diffusivity of the dirtier band, while the initial slope of $H_{c2}(T)$ is determined by that of the cleaner band. Carbon doping of MgB_2 appears to be particularly valuable to enhancing H_{c2} [90], [98], [99]. One effective way of both enhancing H_{c2} and the flux pinning strength may be by the addition of SiC nanoparticles [100]. Because the fabrication of MgB_2 can occur by conventional metal-working processes, the barrier to experimentation is low. The problems of fabricating MgB_2 conductors commercially are being addressed by Hyper Tech Research, Columbus, OH [101], Columbus Superconductors, Genova, Italy [102], Hitachi, Hitachi City, Japan, and NIMS in Japan [103], and many other laboratories worldwide, as a good recent survey makes clear [12]. Several groups have fabricated more than 100-m lengths of prototype wires. Assuming costs can be kept low, competition with Nb-base LTS conductors seems likely, while competition with either BSCCO-based or YBCO-based first- and second-generation HTS conductors will depend on progress in expanding the

temperature range where high currents are maintained in several tesla fields.

XI. Conclusion

The overall picture of superconductor wire is diverse and developing rapidly. The LTS materials Nb–Ti and Nb_3Sn are well established in high-energy physics, commercial MRI and NMR, and many low-temperature magnet applications. Their properties are well developed and their applications well understood. Even though Nb_3Sn will be 50 years old this year, it has seen great progress recently. The very recently discovered MgB_2 has the potential to play a growing role in these applications. BSCCO-2212 wire also has advantages for ultrahigh magnetic field use. Great changes are likely in the arena of electric power applications and magnet applications at temperatures above 30 K. Here the HTS materials BSCCO-2223 and YBCO are the strongest candidates, with first-generation HTS wire based on BSCCO-2223 already commercially available and applied in a variety of prototypes. Indeed, the first commercial sale of HTS power equipment based on first-generation HTS wire has recently occurred for dynamic synchronous condensers supplying reactive compensation in the power grid [104]. This is a harbinger of a coming revolution in the market for superconductor wire.

References

[1] B. Seeber, Ed., "Commercially available superconducting wires," in *Handbook of Applied Superconductivity*, Bristol, U.K.: Inst. of Physics, 1998, pp. 397–488.

[2] B. Seeber, Ed., "Present applications of superconductivity," in *Handbook of Applied Superconductivity*, Bristol, U.K.: Inst. of Physics, pp. 1165–1484.

[3] L. Masur, "Industrial high temperature superconductors: Perspectives and milestones," *IEEE Trans. Appl. Superconduct.*, vol. 12, pp. 1145–1150, Mar. 2002.

[4] B. Seeber, Ed., "Power applications of superconductivity," in *Handbook of Applied Superconductivity*, Bristol, U.K.: Inst. of Phys., 1998, pp. 1485–1756.

[5] S. Kalsi *et al.*, "Installation and operation of superconducting rotating machines," presented at the IEEE Transmission and Distribution Meeting, Dallas, TX, 2003.

[6] B. W. McConnell, M. S. Walker, and S. Mehta, "HTS transformers," *IEEE Power Eng. Rev.*, vol. 20, pp. 7–11, June 2000.

[7] A. P. Malozemoff, J. Maguire, B. Gamble, and S. Kalsi, "Power applications of high temperature superconductors: Status and perspectives," *IEEE Trans. Appl. Superconduct.*, vol. 11, pp. 778–781, Mar. 2002.

[8] H. W. Weijers *et al.*, "The generation of 25.05 T using a 5.11 T $Bi_2Sr_2CaCu_2O_x$ superconducting insert magnet," *Supercond. Sci. Technol.*, vol. 17, pp. 636–644, 2004.

[9] D. Larbalestier, A. Gurevich, D. M. Feldmann, and A. Polyanskii, "High T_c superconducting materials for electric power applications," *Nature*, vol. 414, pp. 368–377, 2001.

[10] A. P. Malozemoff *et al.*, "HTS wire: Status and prospects," *Physica C*, vol. 386, pp. 424–430, 2003.

[11] M. Gouge *et al.*, Advances in Cryogenic Engineering. Melville, NY: AIP, 2004, to be published.

[12] R. Flukiger *et al.*, "Superconducting properties of MgB_2 tapes and wires," *Physica C*, vol. 385, pp. 286–305, 2003.

[13] (2001, May) National Energy Policy: Report of the National Energy Policy Development Group. [Online]. Available: http://www.whitehouse.gov/energy

[14] (2002, May) National Transmission Grid Study. U.S. Dept. Energy. [Online]. Available: http://tis.eh.doe.gov/ntgs/reports

[15] Grid 2030: A national vision for electricity's second 100 years (2003, July). [Online]. Available: http://www.electricity.doe.gov/vision

[16] M. Wilson, *Superconducting Magnets*, Oxford, UK: Clarendon, 1983.

[17] M. Tinkham, *Introduction to Superconductivity*. New York, NY: McGraw Hill Inc., 1975.

[18] K. A. Mueller *et al.*, "The development of superconductivity research in oxides," in *Proc. 10th Anniversary HTS Workshop*, B. Batlogg *et al.*, Eds., 1996, pp. 3–16.

[19] A. P. Malozemoff, "Macroscopic magnetic properties of high temperature superconductors," in *Physical Properties of High Temperature Superconductors*, D. Ginsburg, Ed, Singapore: World Scientific, 1989, pp. 71–150.

[20] ——, "Flux creep in high temperature superconductors," *Physica C*, vol. 185–189, pp. 264–269, 1991.

[21] ——, "New developments in flux creep of high temperature superconductors," in *AIP Conf. Proc.*, vol. 219, Y.-H. Kao *et al.*, Eds., 1991, p. 84.

[22] R. M. Scanlan, W. A. Fietz, and E. F. Koch, "Flux pinning centers in superconducting Nb_3Sn," *J. Appl. Phys.*, vol. 46, pp. 2244–2249, 1975.

[23] A. Gurevich and A. Pashitskii, "Current transport through low-angle grain boundaries in high-temperature superconductors," *Phys. Rev. B*, vol. 57, pp. 13 878–13 893, 1998.

[24] D. Dimos, P. Chaudhari, and J. Mannhart, "Superconducting transport properties in $YBa_2Cu_3O_{7-\delta}$ bicrystals," *Phys. Rev. B*, vol. 41, pp. 4038–4049, 1990.

[25] N. F. Heinig, R. D. Redwing, J. E. Nordman, and D. C. Larbalestier, "Strong to weak coupling transition in low misorientation angle thin film $YBa_2Cu_3O_{7-\delta}$ bicrystals," *Phys. Rev. B*, vol. 60, pp. 1409–1417, 1999.

[26] D. T. Verebelyi *et al.*, "Low angle grain boundary transport in $YBa_2Cu_3O_{7-\delta}$ coated conductors," *Appl. Phys. Lett.*, vol. 76, pp. 1755–1757, 2000.

[27] A. P. Malozemoff, G. N. Riley, S. Fleshler, and Q. Li *et al.*, "Supercurrent conduction mechanisms in BSCCO-2223 tapes," in *Proc. Int. Workshop Critical Currents In Superconductors for Practical Applications*, Y. H. Kao *et al.*, Eds., 1998, pp. 32–39.

[28] B. Hensel, G. Grasso, and R. Flukiger, "Aspects of the current understanding of the supercurrent transport in $(Bi,Pb)_2Sr_2Ca_2Cu_3O_{10-x}$ silver-sheathed tapes—The 'railway-switch' model," *J. Electron. Mater.*, vol. 24, pp. 1877–1881, 1995.

[29] H. Wada, L. F. Goodrich, C. Walters, and K. Tachikawa, Eds., *IEC 61 788-1 (1998–02), Superconductivity—Part 1: Critical Current Measurement—DC Critical Current of Cu/Nb–Ti Composite Superconductors, IEC 61 788-2 (1999–03), Superconductivity—Part 2: Critical Current Measurement—DC Critical Current of Nb_3Sn Composite Superconductors*.

[30] L. A. Schwartzkopf *et al.*, "The use of the in-field critical current density, Jc(0.1 T), as a better descriptor of $(Bi,Pb)_2Sr_2Ca_2Cu_3O_x$/Ag tape performance," *Appl. Phys. Lett.*, vol. 75, pp. 3168–3170, 1999.

[31] G. Stejic *et al.*, "Effect of geometry on the critical currents of thin films," *Phys. Rev. B*, vol. 49, pp. 1274–1288, 1994.

[32] A. A. Polyanskii *et al.*, "Magneto-optical studies of the uniform critical state in bulk MgB_2," *Supercond. Sci. Technol.*, vol. 14, pp. 811–815, 2001.

[33] J. M. Rowell, "The widely variable resistivity of MgB_2 samples," *Supercond. Sci. Technol.*, vol. 16, pp. R17–R27, 2003.

[34] M. N. Wilson, C. R. Walters, J. D. Lewin, and P. F. Smith, "Experimental and theoretical studies of filamentary superconducting composites," *J. Physics D, Appl. Phys.*, vol. 3, pp. 1517–1583, 1970.

[35] D. C. Larbalestier *et al.*, "High critical current densities in industrial scale composites made from high homogeneity Nb 46.5 Ti," *IEEE Trans. Mag.*, vol. 21, pp. 269–272, Mar. 1985.

[36] D. C. Larbalestier, L. Chengren, W. Starch, and P. J. Lee, "Limitation of critical current density by intermetallic formation in fine filament Nb–Ti superconductors," *IEEE Trans. Nucl. Sci.*, vol. NS-32, pp. 3743–3745, 1985.

[37] M. T. Taylor *et al.*, "Co-processed Nb–25% Zr/Cu composite," *Cryogenics*, vol. 11, pp. 224–226, 1971.

[38] E. Gregory, T. S. Kreillick, A. K. Ghosh, and W. B. Sampson, "Importance of spacing in the development of high current densities in multifilamentary superconductors," *Cryogenics*, vol. 27, pp. 178–182, 1987.

[39] A. W. West, W. H. Warnes, D. L. Moffat, and D. C. Larbalestier, "Compositional inhomogeneities in Nb–Ti and its alloys," *IEEE Trans. Magn.*, vol. 19, pp. MAG-749–753, May 1983.

[40] P. J. Lee and D. C. Larbalestier, "Development of nanometer scale structures in composites of Nb–Ti and their effect on the superconducting critical current density," *Acta Metallurgica*, vol. 35, pp. 2523–2536, 1987.

[41] L. Chengren and D. C. Larbalestier, "Development of high critical current densities in niobium 46.5 wt% titanium," *Cryogenics*, vol. 27, pp. 171–177, 1987.

[42] G. L. Dorofejev, E. Yu. Klimenko, and S. V. Frolov, "Artificial pinning centers," in *Proc. 9th Conf. Magnet Technology*, C. Marinucci and P. Weymuth, Eds., 1985, pp. 564–566.

[43] L. D. Cooley and L. R. Motowidlo, "Advances in high field superconducting composites by addition of artificial pinning centers to niobium-titanium," *Supercond. Sci. Technol.*, vol. 12, pp. R135–R151, 1999.

[44] L. R. Motowidlo, M. K. Rudziak, and T. Wong, "The pinning strength and upper critical fields of magnetic and nonmagnetic artificial pinning centers in Nb47wt%Ti wires," *IEEE Trans. Appl. Superconduct.*, vol. 13, pp. 3351–3354, June 2003.

[45] O. V. Chernyi *et al.*, "The microstructure and critical current density of Nb-48wt%Ti superconductor with very high alpha-Ti precipitate volume and very high critical current," *Adv. Cryogenic Eng.*, vol. 48, no. B, pp. 883–890, 2002.

[46] ITER Web page [Online]. Available: http://www.iter.org

[47] N. Mitchell *et al.*, "Strand production and benchmark testing for the ITER model coils," *IEEE Trans. Appl. Superconduct.*, vol. 5, pp. 905–908, June 1995.

[48] R. M. Scanlan, "Conductor development for high energy physics—Plans and status of the U.S. program," *IEEE Trans. Appl. Superconduct.*, vol. 11, pp. 2150–2155, Mar. 2001.

[49] J. A. Parrell, M. B. Field, Y. Zhang, and S. Hong, "Nb_3Sn conductor development for fusion and particle accelerator applications," *Adv. Cryogenic Mater.*, vol. 50, 2004, to be published.

[50] A. F. Lietzke *et al.*, "Test results for HD1, a 16 T Nb_3Sn dipole magnet," *IEEE Trans. Appl. Superconduct.*, vol. 14, 2004, to be published.

[51] P. J. Lee *et al.*, "The microstructure and microchemistry of high critical current Nb_3Sn strands manufactured by the bronze, internal-Sn, and PIT techniques," *IEEE Trans. Appl. Superconduct.*, vol. 13, pp. 3422–3425, June 2003.

[52] J. Lindenhovius *et al.*, "Powder-in-tube (PIT) Nb_3Sn conductors for high field magnets," *IEEE Trans. Appl. Superconduct.*, vol. 10, pp. 975–978, Mar. 2000.

[53] K. Okuno *et al.*, "Test of the NbAl insert and ITER central solenoid model coil," *IEEE Trans. Appl. Superconduct.*, vol. 13, pp. 1437–1440, June 2003.

[54] T. Takeuchi, "Nb_3Al conductors for high-field applications," *Supercond. Sci. Technol.*, vol. 13, pp. R101–R119, 2000.

[55] N. Banno *et al.*, "Multifilamentary Nb/Al-Ge and Nb/Al-Si precursor fabrication using the intermediately rapid heating and quenching technique," *Supercond. Sci. Technol.*, vol. 17, pp. 320–326, 2004.

[56] F. Buta, M. D. Sumption, and E. W. Collings, "Influence of transformation heat treatment on microstructure and defects in RHQT-processed Nb_3Al," *IEEE Trans. Appl. Superconduct.*, vol. 13, pp. 3458–3461, June 2003.

[57] T. Hasegawa *et al.*, "High J_c Bi-2212/Ag multilayer tape conductor prepared by a coating method," in *Advances in Superconductivity XII*, T. Yamashita and K. Tanabe, Eds, Tokyo, Japan: Springer-Verlag, 2000, pp. 640–645.

[58] H. W. Weijers *et al.*, "Development and testing of a 3 T Bi-2212 insert magnet for high field NMR," *IEEE Trans. Appl. Superconduct.*, vol. 9, pp. 563–566, June 1999.

[59] T. Kiyoshi *et al.*, "Generation of 23.4 T using two Bi-2212 insert coils," *IEEE Trans. Appl. Superconduct.*, vol. 10, pp. 472–477, Mar. 2000.

[60] Y. Aoki *et al.*, "A high-T_c superconducting Rutherford cable uing Bi-2212 oxide superconducting round wire," in *Advances in Superconductivity XII*, T. Yamashita and K. Tanabe, Eds, Tokyo, Japan: Springer-Verlag, 2000, pp. 827–829.

[61] R. Gupta *et al.*, "Status of high temperature superconductor magnet R&D at BNL," *IEEE Trans. Appl. Superconduct.*, vol. 13, pp. 1351–1354, June 2003.

[62] C.-E. Bruzek *et al.*, "High-performance Bi2212/Ag tape produced at Nexans," *Supercond. Sci. Technol.*, 2004, to be published.

[63] S. Patnaik *et al.*, "Local measurement of current density by magneto-optical current reconstruction in normally and overpressure processed Bi-2223 tapes," *IEEE Trans. Appl. Superconduct.*, vol. 13, pp. 2930–2933, June 2003.

[64] Y. B. Huang *et al.*, "Improving the critical current density in Bi-2223 wires via a reduction of the secondary phase content," *IEEE Trans. Appl. Superconduct.*, vol. 13, pp. 3038–3041, June 2003.

[65] Y. Yuan *et al.*, "Overpressure processing of Ag-sheathed $(Bi,Pb)_2Sr_2Ca_2Cu_3O_x$ tapes," *Physica C*, vol. 372–376, pp. 883–886, 2002.

[66] Y. Yuan *et al.*, "Significantly enhanced critical current density in Ag-sheathed $(Bi,Pb)_2Sr_2Ca_2Cu_3O_{10-x}$ composite conductors prepared by overpressure processing," *Appl. Phys. Lett.*, vol. 84, pp. 2127–2129, 2004.

[67] Y. Iijima *et al.*, "Reel to reel continuous formation of Y-123 coated conductors by IBAD and PLD," *IEEE Trans. Appl. Superconduct.*, vol. 11, pp. 2816–2821, Mar. 2001.

[68] X. D. Wu *et al.*, "Properties of $YBa_2Cu_3O_{7-\delta}$ thick-films on flexible buffered metallic substrates," *Appl. Phys. Lett.*, vol. 67, pp. 2397–2399, 1995.

[69] A. Usoskin *et al.*, "Large area YBCO-coated stainless steel tapes with high critical currents," *IEEE Trans. Appl. Superconduct.*, vol. 13, pp. 2452–2457, June 2003.

[70] S. R. Foltyn *et al.*, "Strongly coupled critical current density values achieved in $YBa_2Cu_3O_{7-\delta}$ coated conductors with near-single-crystal texture," *Applied Physics Letters*, vol. 82, pp. 4519–4521, 2003.

[71] T. Izumi, Y. Yamada, and Y. Shiohara, "All Japan efforts on R&D of HTS coated conductors for future applications," *Physica C*, vol. 392–396, pp. 9–16, 2003.

[72] A. Goyal *et al.*, "High critical current density superconducting tapes by epitaxial deposition of $YBa_2Cu_3O_x$ thick films on biaxially textured metals," *Appl. Phys. Lett.*, vol. 69, pp. 1795–1797, 1996.

[73] A. Goyal *et al.*, "Recent progress in the fabrication of high-J_c tapes by epitaxial deposition of YBCO on RABiTS," *Physica C*, vol. 357–360, pp. 903–913, 2001.

[74] K. Ohmatsu *et al.*, "Development of in-plane aligned YBCO tapes fabricated by inclined substrate deposition," *Physica C*, vol. 357–360, pp. 946–951, 2001.

[75] A. P. Malozemoff *et al.*, "Low-cost YBCO coated conductor technology," in *IOP Conf. Series*, vol. 167, London, 2000, pp. 307–312.

[76] D. Verebelyi *et al.*, "Practical neutral axis conductor geometries for coated conductor composite wire," *Superconductor Science and Technology*, vol. 16, pp. 1158–1161, 2003. ibid, "Uniform performance of continuously processed MOD-YBCO coated conductors using a textured Ni-W substrate,"*Supercond. Sci. and Technol.*, pp. L19–L23, vol. 16, 2003.

[77] C. P. Wang *et al.*, "Deposition of in-plane textured MgO on amorphous Si_3N_4 substrates by ion-beam-assisted deposition and comparison with ion-beam-assisted deposition yttria-stabilized-zirconia," *Appl. Phys. Lett.*, vol. 71, pp. 2955–2957, 1997.

[78] R. Metzger, "Superconducting tapes using ISD buffer layers produced by evaporation of MgO or reactive evaporation of magnesium," *IEEE Trans. on Applied Superconductivity*, vol. 11, pp. 2826–2829, Mar. 2001.

[79] B. Ma *et al.*, "High critical current density of YBCO coated conductors fabricated by inclined substrate deposition," *Physica C*, vol. 403, pp. 183–190, 2004.

[80] R. P. Reade, P. Berdahl, R. E. Russo, and S. M. Garrison, "Laser deposition of biaxially textured yttria-stabilized zirconia buffer layers on polycrystalline metallic alloys for high critical current Y-Ba-Cu-O thin films," *Appl. Phys. Lett.*, vol. 61, pp. 2231–2233, 1992.

[81] V. Selvamanickam, H. G. Lee, Y. Li, X. Xiong, Y. Qiao, J. Reeves, Y. Xie, A. Knoll, and K. Lenseth, "Fabrication of 100 A class, 1 m long coated conductor tapes by metal organic chemical vapor deposition and pulsed laser deposition," *Physica C*, pp. 392–396, 859–862, 2003.

[82] D. M. Feldmann *et al.*, "Through-thickness superconducting and normal-state transport properties revealed by thinning of thick film ex situ $YBa_2Cu_3O_{7-\delta}$ coated conductors," *Appl. Phys. Lett.*, vol. 83, pp. 3951–3953, 2003.

[83] A. P. Malozemoff. (2004) Second Generation HTS Wire: An Assessment. [Online]. Available: http://www.amsuper.com/html/products/library/2g_white_paper_-_march_2002.pdf

[84] J. Nagamatsu *et al.*, "Superconductivity at 39 K in magnesium diboride," *Nature*, vol. 410, pp. 63–64, 2001.

[85] H. J. Choi *et al.*, "The origin of anomalous superconducting properties of MgB_2," *Nature*, vol. 418, pp. 758–760, 2002.
[86] A. Gurevich, "Enhancement of H_{c2} by nonmagnetic impurities in dirty two-gap superconductors," *Phys. Rev. B*, vol. 67, pp. 185 415–13, 2003.
[87] A. Gurevich *et al.*, "Very high upper critical fields in MgB_2 produced by selective tuning of impurity scattering," *Supercond. Sci. Technol.*, vol. 17, pp. 278–286, 2004.
[88] D. C. Larbalestier *et al.*, "Strongly linked current flow in polycrystalline forms of the new superconductor MgB_2," *Nature*, vol. 410, pp. 186–189, 2001.
[89] *Physica C*, vol. 385, no. 1–2, pp. 1–385, Mar. 2003. A broad review of recent work on MgB_2.
[90] V. Braccini *et al.*. (2004) High-field superconductivity in alloyed MgB_2 thin films. *Condens. Matter* [Online]. Available: http://arxiv.org/pdf/cond-mat/0402002
[91] W. Goldacker *et al.*, "Considerations on critical currents and stability of MgB_2 wires made by different preparation routes," *Physica C*, vol. 401, pp. 80–86, 2004.
[92] R. F. Klie *et al.*, "Observation of coherent oxide precipitates in polycrystalline MgB_2," *Appl. Phys. Lett.*, vol. 80, p. 3970, 2002.
[93] X. Song, V. Braccini, and D. Larbalestier, "Inter- and intra-granular nanostructure and possible spinodal decomposition in low resistivity bulk MgB_2 with varying critical fields," *J. Mater. Res.*, 2004, to be published.
[94] S. Y. Xu *et al.*, "High critical current density and vortex pinning of epitaxial MgB_2 thin films," *Phys. Rev. B.*, vol. 68, pp. 224 501–224 508, 2003.
[95] V. Braccini and D. C. Larbalestier, unpublished work.
[96] L. D. Cooley and R. M. Scanlan, private communication.
[97] Y. Ando *et al.*, "Resistive upper critical fields and irreversibility lines of optimally doped high-T_c cuprates," *Phys. Rev. B*, vol. 60, pp. 12 475–12479, 1999.
[98] R. H. T. Wilke *et al.*. (2003) Systematic effects of carbon doping on the superconducting properties of $Mg(B_{1-x}C_x)_2$. *Condens. Matter Archive* [Online]. Available: http://arxiv.org/abs/cond-mat/0312235
[99] E. Ohmichi, T. Masui, S. Lee, S. Tajima, and T. Osada. (2003) Enhancement of the irreversibility field by carbon substitution in single crystal MgB_2. *Condens. Matter Archive* [Online]. Available: http://arxiv.org/abs/cond-mat/0312348
[100] S. X. Dou *et al.*, "Enhancement of the critical current density and flux pinning of MgB_2 superconductor by nanoparticle SiC doping," *Appl. Phys. Lett.*, vol. 81, pp. 3419–3421, 2002.
[101] S. Soltanian *et al.*, "Transport critical current of solenoidal MgB_2/Cu coils fabricated using a wind-reaction in situ technique," *Supercond. Sci. Technol.*, vol. 16, pp. L4–L6, 2003.
[102] G. Grasso *et al.*, "Fabrication and properties of monofilamentary MgB_2 superconducting tapes," *Supercond. Sci. Technol.*, vol. 16, pp. 271–275, 2003.
[103] A. Matsumoto, H. Kumakura, H. Kitaguchi, and H. Hatakeyama, "Effect of impurity additions on the microstructures and superconducting properties of in situ-processed MgB_2 tapes," *Supercond. Sci. Technol.*, vol. 17, pp. S319–S323, 2004.
[104] S. Kalsi *et al.*, "Superconducting dynamic synchronous condenser for improved grid voltage support," presented at the IEEE Transmission and Distribution Conf., Dallas, TX, 2003.

Ronald M. Scanlan received the Ph.D. degree from Cornell University, Ithaca, NY, in 1970.

Earlier in his career, he was responsible for development of Nb_3Sn conductor for the HFTF fusion magnet at the Lawrence Livermore National Laboratory. He was the Group Leader for Superconducting Wire and Cable Development at the Lawrence Berkeley National Laboratory (LBNL), Berkeley, CA. At LBNL (1994–1999), he also served as the Magnet Program Head during the design, construction, and testing of the world's first 13.5-T Nb_3Sn dipole magnet. Most recently, he managed the Conductor Development Program for the Division of High Energy Physics, U.S. Department of Energy, Washington, DC. The goal of this program is the industrial development of a cost-effective, high-field superconductor for accelerator magnet applications. In the first 18 months of this program, one of the participating industrial firms was able to increase the critical current density in Nb_3Sn by over 50%, to 3000 A/mm^2 at 4.2 K and 12 T. He is currently retired. He is the author or coauthor of over 100 publications in the field of superconducting materials.

Dr. Scanlan shared the IEEE Particle Accelerator Conference Award for 1991 with Dr. D. C. Larbalestier "for the development of NbTi superconducting material for high current density application in high field superconducting magnets."

Alexis P. Malozemoff (Senior Member, IEEE) received the B.A. degree from Harvard University, Cambridge, MA, in 1966 and the Ph.D. degree from Stanford University, Stanford, CA, in 1970.

He was with IBM Research, Yorktown Heights, NY. He is currently Executive Vice President and Chief Technical Officer of American Superconductor Corporation, Westborough, MA. He is responsible for research and development strategy, advanced conductor development, and the intellectual property portfolio. He has more than 20 years of experience in superconducting materials and systems, as well as in magnetic materials and devices. He has numerous publications and patents in magnetism and superconductivity.

Dr. Malozemoff is a Fellow of the American Physical Society.

David C. Larbalestier received the Ph.D. degree from Imperial College, London, U.K., in 1970.

He worked in the Superconducting Magnet Research Group of the Rutherford Laboratory in 1972–1976 on the first multifilamentary Nb_3Sn conductors and magnets. He joined the University of Wisconsin, Madison, in 1976, where he is currently Professor in the Departments of Materials Science and Engineering and of Physics, where he holds both the L. V. Shubnikov Chair and the Grainger Chair of Superconductivity and is also the Director of the Applied Superconductivity Center. He has been active in superconductivity since he was working toward his Ph.D. degree. His group has had a large influence on the understanding and application of both low and high temperature superconductors.

Dr. Larbalestier is a Fellow of the American Physical Society and the Institute of Physics and a Member of the National Academy of Engineering. His Ph.D. work gained the Matthey Prize of Imperial College. He shared a 1978 IR-100 award with an Oxford Instrument team for their work on the first Nb_3Sn NMR magnet. His work has been recognized by the 1991 IEEE Particle Accelerator Conference Award (jointly with R. M. Scanlan) and the 2000 IEEE Award for continuing and significant contributions in the field of applied superconductivity, and by the Council for Chemical Research (2000) for work by him and his collaborators on $(Bi,Pb)_2Sr_2Ca_2Cu_3O_x$.